Biosorption of nonylphenol on dead biomass of *Rhizopus arrhizus* encapsulated in chitosan beads.

Weeranuch Lang[1,*], Chomawan Dejma[1], Sarote Sirisansaneeyakul[2], Nobuo Sakairi[3]

[1]Department of Microbiology, Faculty of Liberal Arts and Science, Kasetsart University, Kampaeng Saen, Nakorn-Pathom 73140, Thailand

[2]Department of Biotechnology, Faculty of Agro-Industry, Kasetsart University 10900, Thailand

[3]Graduate School of Environmental Science, Hokkaido University, Kita-ku, Sapporo 060-0810, Japan

*Corresponding author. Department of Microbiology, Faculty of Liberal Arts and Science, Kasetsart University, Nakorn-Pathom 73140, Thailand. Tel.: +6634-281-105-7; fax: +6634-281-057.

E-mail address: faaswnp@ku.ac.th (W. Lang).

Abstract

The nonylphenol (NP) biosorption and desorption potential for fungal biomass used under batch conditions was investigated using kinetics and isotherm models. Fungal biomass of *Rhizopus arrhizus* TISTR 3610 exhibited preferential uptake of NP, an endocrine disrupting chemicals. Sporangiospores, asexual spores, were immobilisation in chitosan beads. The biosorption data of NP on the moist heat inactivated *R. arrhizus*-chitosan beads were analyzed using four popular adsorption isotherms and, by using non-linear least-regression with the *solver* add-in in Microsoft Excel, correlated in order with the Fritz-Schlüender > Redlich-Peterson > Freundlich > Langmuir isotherms. The pseudo first-order kinetics was found to have the best fit with the experimental data. The diffusivity of NP in the *R. arrhizus*-chitosan beads was calculated using the shrinking core model, and the diffusivity values were in the ranges of 2.3736×10^{-4} to 1.8950×10^{-4} $cm^2 s^{-1}$. Desorption to recover the adsorbed NP from the beads was performed in methanol and was best described using a pseudo second-order kinetic model.

Keywords: Biosorption; Nonylphenol; *Rhizopus arrhizus*; Chitosan; kinetic modelling

List of Symbols

V	volume of aqueous phase (L)
M	mass of biomass (g)
a_S	Fritz-Schlüender isotherm constant $(mg/L)^{-b2}$
a_R	Redlich-Peterson isotherm constant $(L/mg)^{\beta}$
b	Langmuir isotherm constant (L/mg)
b_1, b_2	Fritz-Schlüender isotherm constants (dimensionless)
C	concentration of NP at time, t (ppm)
C_0	initial concentration of NP (ppm)
C^0	$\frac{(C_0-C_e)V}{n\frac{4}{3}\pi R^3}$, average NP binding site density (ppm)
C_e	concentration of NP at equilibrium (ppm)
D	diffusion coefficient (cm^2/s)
K_1	Pseudo first-order rate constant (min^{-1})
K_2	Pseudo second-order rate constant modified (g/mg min)
k_p	intraparticle diffusion rate constant ($mg/g\ min^{0.5}$)
K_F	Freundlich constant, characteristic of the system related to the adsorption capacity (mg/g)
K_R	Redlich-Peterson isotherm constant (L/g)
K_S	Fritz-Schlüender isotherm constant $(mg/g)\ (mg/L)^{-b1}$
n	Freundlich constant, characteristic of the system related to the adsorption intensity (dimensionless)
q	NP uptake rate (mg/g)
q_e	NP uptake rate at equilibrium (mg/g)
Q_0	Langmuir adsorption isotherm constant (mg/g) (Dependent on the

	maximum adsorption capacity of biosorbent)
R	radius of bead (cm)
t	contact time (min)
X, $F(X)$	Functions derived from the shrinking core model (Preetha and Viruthagirl, 2007)
RMS	root mean square
q_{cal}	theoretical NP uptake (mg/g)
q_{exp}	experimental NP uptake (mg/g)
K_D	desorption rate constant (s^{-1})

Greek letters

α	$\int_0^t Cdt$, derived from the shrinking core model, defined in Eq.(13) and (14) (Preetha and Viruthagirl, 2007)
α_P	Redlich-Peterson isotherm constant
β	Redlich-Peterson isotherm constant (Dependent on the heterogeneity of the binding surface)

1. Introduction

Nonylphenol (NP) is one of the organic pollutants found in aquatic environments as a consequence of the biodegradation of nonylphenol polyethoxylate (NPnEO), a non-ionic surfactant contained in industrial cleaning products and in household detergents (Ahel *et al*., 1993). Although the parent surfactant itself is less toxic, NPnEO released into the environment rapidly decomposes to form NP which is the most recalcitrant intermediate of NPnEO decomposition. Principally NP persists in sewage treatment plants and outflows (Nakada *et al*., 2006), and tends to accumulate in the fatty tissue of aquatic organisms when released into aquatic environments.

NP is known to be an endocrine disruptor compound, that is, it mimics endogenous hormones and disrupts important life processes. Substantial evidence exists to demonstrate that NP causes various disorders of the male reproductive system, including reduced testicular size and lower sperm production in rainbow trout and other marine animals (Granmo *et al*., 1989; Ekelund *et al*., 1990). NP and NPnEO have been banned in the European Union as a hazard to human and environmental safety. However, NP and NPnEO are still widely used in Thailand and other Asian countries, especially as industrial detergents such as those used for wool washing and metal finishing, in various laboratory detergents including Titron X-100, in industrial processes such as emulsion polymerisation, and in some pesticide formulations.

Although the techniques of adsorption on activated carbon, photo-oxidation and ozone treatment for NP removal have been studied and found to be effective, cost-effectiveness is the main limitation against widespread practical use (Nevskaia and Guerrero, 2001; Kawasaki *et al*., 2001). The search for a low cost and easily

available adsorbent has led the authors to investigate materials of agricultural and biological origin, and some industrial by-products as adsorbents.

Biosorption, the passive uptake of pollutants by non-growing or non-living microbial biomass such as bacteria, fungi and algae, is considered to have good potential for the removal of non-degradable pollutants from aqueous solution (Kapoor and Viraraghavan, 1995). Reports of biosorption of toxic organic compounds with biomass showed that better removal was obtained with dead biomass than with live biomass (Aksu, 2005). Immobilisation may also allow higher biomass concentrations, and facilitate separation and non-destructive recovery of biomass from pollutant-bearing solution (Fu and Viraraghavan, 2001). Immobilised fungal biomass has been used for the removal of various metals, dyes and some organic pollutants (Kapoor and Viraraghavan, 1995; Aksu, 2005) but no study has been conducted on the use of immobilised biomass for the removal of NP or other endocrine disruptor compounds. Therefore, there is a need to study the performance of the immobilised fungus system with NP.

Chitosan, (1→4)-2-amino-2-deoxy-β-D-glucan, produced on an industrial scale by the alkaline deacetylation of chitin, one of the most abundant biopolymers in nature, was used in this study as the supporting material for living biomass immobilisation. It should be noted that the use of chitosan for living cell immobilisation has a limitation due to its anti-microbial activity (Helander *et al*., 2001). However, the fungal resting spores used in this study are tolerant to chitosan gelling because of their extra thick cell wall.

This study presents the biosorption characteristics of NP on dead chitosan-immobilised fungal beads, referred to as “dead beads”. Suitable isotherm and kinetic models fitted by non-linear regression using the ‘*solver’* add-in with Microsoft Excel

2007 are proposed. Also, the reusability of the dead beads, that is the stability to repeated adsorption-desorption cycles, is discussed in reference to their feasibility for industrial use.

1.1 Adsorption equilibrium

The capacity of an adsorbent can be described by the equilibrium sorption isotherm, which is characterised by certain constants whose values express the surface properties and affinity of the adsorbent.

1.1.1 The Langmuir sorption isotherm

This model assumes an ideal, totally homogeneous adsorption surface with a finite number of binding sites and a few interactions between adsorbed molecules (Aksu and Balibek, 2007) is given by:

$$q = \frac{Q_0 b C_e}{1 + b C_e} \quad (1)$$

1.1.2 The Freundlich sorption isotherm

This model is suitable for a highly heterogeneous, energetic distribution of active sites, with interactions between adsorbed molecules (Aksu, 2001; Aksu *et al*., 2007), and is given by:

$$q = K_F C_e^{1/n} \quad (2)$$

1.1.3 The Redlich-Peterson sorption isotherm

This model is a combination of the Langmuir and Freundlich models and is given by Eq.(3). β lies between 0 and 1. For β = 1 the Redlich-Peterson model converts to the Langmuir model (Aksu, 2001).

$$q = \frac{K_R C_e}{1 + a_R C_e^{\beta}} \quad (3)$$

1.1.4 The Fritz-Schlüender sorption isotherm

This isotherm for single-component systems more flexible to fit the experimental data since it contains more parameters than any other equilibrium isotherm (Fritz-Schlüender, 1974; Yang and Al-Duri, 2005). It is usually written as:

$$q = \frac{K_S C_e^{b1}}{1 + a_S C_e^{b2}} \quad (4)$$

1.2 Adsorption kinetics

1.2.1 Kinetic models

Two simplified kinetic equations, from the pseudo first-order and pseudo second-order kinetic models initially proposed by Lagergren (1989) and Ho and McKay (2000) respectively, were used for a wide range of solute-sorbent systems.

1.2.1.1 Pseudo first-order kinetic model (Lagergren's equation)

This model assumes that the biosorption rate is proportional to the number of unoccupied sites on the biosorption surface (Ozdemir et *al*., 2003). The kinetic model based on solid capacity gives:

$$q = q_e\left(1 - e^{-K_1 t}\right) \quad (5)$$

1.2.1.2 Pseudo second-order kinetic model (Ho's equation)

This model assumes the driving force for adsorption rate comes from the square of the difference between q and q_e. It was transformed to non-linear form, giving as the equation:

$$q = \frac{q_e^{\,2} K_2 t}{1 + q_e K_2 t} \quad (6)$$

1.2.2 Diffusion models

Sorption kinetics is generally controlled by various factors including (i) bulk diffusion, (ii) film diffusion (external mass transfer), (iii) intraparticle diffusion, and (iv) solute adsorption at active sites by the mechanisms of ion exchange, precipitation, complexation or chelation. Different diffusion models propose different diffusion kinetic mechanisms and rate-controlling steps.

1.2.2.1 Intraparticle diffusion model

The model implies that the diffusion from the surface to intraparticle sites is the only rate-limiting step (Yang and Al-Duri, 2005). The model can be expressed as:

$$q = k_p t^{0.5} \quad (7)$$

The half adsorption time $t^{0.5}$ is the time required for the adsorbent to take up half of the adsorbate it has at equilibrium. The rate constant, k_p obtained from the slope of Eq. (11), is related to the intraparticle diffusivity as:

$$k_p = \frac{6q_e}{R}\sqrt{\frac{D}{\pi}} \quad (8)$$

1.2.2.2 Shrinking core model

This model was applied to fluid-particle chemical reactions (Levenspiel, 1972) and, more specifically, to solute adsorption by ion exchange, precipitation, complexation and/or chelation. These processes are controlled by liquid film diffusion, with the extent of the sorption being a function of time given by:

$$X = \frac{3D}{\delta RC}\alpha \quad (9)$$

If the film diffusion is the rate determining process, a plot of X versus α will give a straight line (Preetha and Viruthagirl, 2007). If the process is the particle diffusion control, the model is represented by:

$$F(X) = 1-3(1-X)^{2/3}+2(1-X) = \frac{6D}{R^2C_0}\alpha \quad (10)$$

Consequently, in this case, a plot of the function *F(X)* versus α will give a linear relationship, and the diffusivity can be obtained from the slope of such a plot using (Preetha and Viruthagirl, 2007):

$$D = (slope)\frac{C^0R^2}{6} \quad (11)$$

3. Materials and Methods

3.1 Materials

3.1.1 Chemicals

NP was purchased from Fluka Chemical Industries, Ltd. It was a mixture of isomers and used without further purification. Chitosan was a gift from TC Union Company, Thailand. All other chemicals used were of reagent grade.

3.1.2 Microorganisms

Five fungal strains, i.e. *R. arrhizus* TISTR 3606, *R. Arrhizus* TISTR 3610, *Trichoderma harzanum*, *Aspergillus oryzae* and *Penicillium* sp., available from a microbiological laboratory of Faculty of Liberal Arts and Science, Kasetsart University, were used in this work.

3.1.3 Instruments

Absorbance spectra were recorded on an Ultrospec 3000 UV–Vis spectrometer. Freeze-dried samples were prepared using a Bio-freezer and DW 3 Lyophilyzer (Scientific promotion Co., Ltd.).

3.2 Methods

3.2.1 Preparation of fungal biomass for NP biosorption.

The five fungal strains were inoculated separately into a growth medium, Tryptone glucose yeast extract (TGY), composed of yeast extract (10 g/L), peptone (20 g/L) and dextrose (20 g/L) in distilled deionised water and cultivated in rotary shaking flasks for 4 days. The biomasses were autoclaved at 121.5^{o}C for 15 min and then harvested by filtering through a membrane filter. These were then washed thoroughly with deionised water and freeze-dried. Each sample of dried dead biomass was ground using a mortar and pestle. Particles passing through a 210 μm sieve were used as fungal powder for NP biosorption.

3.2.2 Pre-treatment of biomass

Five-day old living biomass samples, 5 g wet weight, were pre-treated in six different ways: exposure to acid, basic or organic solution, in combination with and without heat treatment as followings: (i) washed and freeze-dried (untreated), (ii) washed and autoclaved for 15 min at 121^{o}C, (iii) immersed in a 1 M H_2SO_4 for 1 hour washed and freeze-dried, (iv) immersed in a 2 N NaOH for 1 hour, washed and autoclaved at 121^{o}C for 15 min, (v) immersed in a 2 N NaOH and autoclaved at 121^{o}C for 15 min, (vi) immersed in a 10% formaldehyde for 1 hour, washed and freeze-dried and (vii) spread on a membrane filter and dried at 50^{o}C for 24 hours. The treated fungal biomass was then dried and ground according to the above method 3.2.1. The NP biosorption ability of pre-treated samples was also compared with activated charcoal and commercial chitosan powder.

3.2.3 Biosorption study

Stock solution of nonyphenol (1.00 g/L) was prepared in methanol and stored under dark conditions. Fungal powder (0.02 g, duplicate samples) was added to 20 ml of the 100 mg/L of NP solubilised in 10% methanol in 125 ml conical flasks. The

flasks were placed on a rotary shaker (100 rpm, 30^{o}C) for 1 hour. Each mixture was filtered through a membrane filter (Whatman No.1), and then extracted with dichloromethane (20 ml) for NP determination. The concentration of NP in the organic layer was determined by comparing absorbance at a wavelength of 275 nm to a standard curve using dichloromethane as a solvent. The NP uptake was calculated by using:

$$q = \frac{(C_0 - C) * V}{M} \qquad (12)$$

In order to optimize the pH for maximum removal efficiency, experiments are conducted in the pH range from 2.0 to 10.0 using 0.02 g of *R. arrhizus* TISTR 3610 biomass with 20 ml of 100 mg nonylphenol/L solutions at room temperature. pH of the adsorbate solution is adjusted to set value with 0.01 M HCl and 0.01 M NaOH at the start of the experiment. It is confirmed through the preliminary experiments that the 6 hour is sufficient to attain equilibrium between adsorbent and adsorbate. Each experiment is repeated twice and mean values are taken.

3.2.4 Preparation of the dead beads

The entrapment of *R. arrhizus* TISTR 3610 sporangiospores produced immobilised fungal bead biosorbents. Chitosan (2 g) was dissolved in acetic acid solution (3%v/v, 9.9 ml), aseptically heated at 100^{o}C for 5 min, then cooled and mixed with the *R. arrhizus* spore suspension (0.1 ml, about 3.7x10^{9} spores/ml). The chitosan suspension was added dropwise to sterilised sodium tri-polyphosphate (2%w/v, 100 ml) and let stand for 3 hours to yield stable 2 mm diameter beads which were washed several times with deionised distilled water. The beads with trapped spores were transferred into TGY medium and incubated on a rotary shaker (100 rpm) at 30^{o}C for 5 days. After this, the chitosan beads with immobilised fungal mycelia

were inactivated by autoclaving at 121^{o}C for 15 min, removed from the medium by filtration, washed with distilled water and freeze-dried.

3.2.5 SEM Studies

The cross-section and surface of the fungus immobilised beads were observed by SEM using the preparation method of Pluemsab *et al*. (2007).

3.2.6 Batch kinetic experiments

Kinetic experiments were performed in continuously stirred flasks (100 rpm at 30^{o}C) containing 100 ml NP solution at different concentrations (50-300 mg/L) and 0.1 g of the dead beads. Optimal solution pH was adjusted to 6.5-7.0, since NP is removed more effectively by *R. arrhizus* TISTR 3610 biomass. 2 ml samples were withdrawn at regular intervals and extracted with dichloromethane (2 ml). The organic layer was collected by centrifuging at 3,500 rpm at 4^{o}C. The residual NP concentration was determined by UV/vis spectroscopy at 275 nm (Ultrospec 3000, Pharmacia Biotech Inc., Thailand). This was done for duplicate samples of each treatment.

The validity of the isotherm and kinetic models were checked by plotting Eq. (1)-(11) with the observed data. The kinetic parameters involved in the models were estimated using non-linear regression analysis. By trial and error, and using the *solver* add-in with Microsoft Excel spreadsheet application, the kinetic parameters were determined by minimising the difference between the experimental data and fitted model.

3.2.7 Desorption studies

Desorption studies were conducted in methanol with equilibrium being reached within 90 min. Initially, a known weight of dead beads was placed in 100 mg/L NP solution overnight, and the NP adsorbed determined from the difference

between the initial and final NP concentration. The beads were separated from the solution by vacuum filtration.

The NP-beads were mixed with methanol and kept in sealed flasks placed in a shaker at 30^{o}C overnight. The amount of NP desorbed was determined by UV/vis absorbance at 275 nm of wavelength. Various desorption kinetic models were considered and compared against the experimental data for fit. The desorption process was repeated five times to check repeatability.

The desorption ratio was calculated from the amount of NP adsorbed on the biomass and the final NP concentration in desorption medium, that is:

$$Desorption\ \ ratio \quad = \quad \frac{Release\ nonylphenol\ (mg)}{Initially\ sorbed\ nonylphenol\ (mg)}\ x\ 100 \qquad (13)$$

3.2.8 Statistical analyses

The fit of kinetic expressions to the experimental data was tested using the value of coefficient of determination, r^2 (Kumar, 2007), which is defined as:

$$r^2 \quad = \quad \frac{\sum (q_{cal} - \bar{q}_{\exp})^2}{\sum (q_{cal} - \bar{q}_{\exp})^2 + \sum (q_{cal} - q_{\exp})^2} \qquad (14)$$

Also used was the non-normalised root mean square (RMS) that weights the actual error at all points (Yang and Al-Duri, 2005), and is defined as:

$$Non-normalized\ RMS \quad = \quad \sqrt{\frac{\sum_{i=1}^{N} (q_{cal} - q_{\exp})^2}{N}} \qquad (15)$$

All statistical data analysis was performed with the help of the toolbox present in Microsoft® Excel (Microsoft Corporation, USA).

4. Results and Discussion

4.1 Screening of fungal biomass for NP biosorption

Five fungal strains, obtained from the culture collection in a laboratory of the Faculty of Liberal Arts and Science, Kasetsart University, were used for the NP biosorption study. Since NP solubility in water is extremely low (5.43 mg/L at 20^{o}C) (Kim *et al*., 2005), it was extracted from the water layer with dichloromethane before analyses. From an initial concentration of 50 mg/L, the amount of NP absorbed in each fungal mycelia was similar, about 69-76%, as follows: 68.8 ± 2.1% for *R. arrhizus* TISTR 3606, 75.9 ± 0.6% for *R. arrhizus* TISTR 3610, 70.6 ± 2.1% for *T. harzanum*, 70.5 ± 0.6% for *A. oryzae*, and 69 ± 4% for *Penicillium* sp. The UV-vis spectra showed decreases in all three main peaks of NP isomer (Fig. 1). The most effective NP absorbent was the mycelia of *R. arrhizus* TISTR 3610, therefore it was selected as a model of the fungal strains for NP biosorption in this work. Also investigated was the use of non-viable and viable *R. arrhizus* biomass to remove phenol and its derivatives from aqueous solutions in batch reactors (Tsezos and Bell, 1989).

4.2 Pre-treatment of fungal biomass and solution pH for NP biosorption

Research has shown that some physical or chemical pre-treatment processes can facilitate more efficient uptake of sorbate as compared to untreated biomass. Six pre-treatments of mycelial biomass of *R. arrhizus* were prepared to observe various chemical and physical effects on both cell walls and intracellular compartments. Heat treatment by autoclave at 121^{o}C for 15 min was found to be the most effective for biosorption with an uptake of 73.7 ± 1.0 mg NP/g (Table 1). Treatments with drying at 50^{o}C for 24 hours or soaking in 10% (v/v) formaldehyde for 1 hour were also fairly effective, with NP uptakes larger than that of untreated biomass at 54 ± 12 mg NP/g.

However, the chemical treatments with strong acid or strong base reduced the NP absorption capacity. It could be concluded that the surface modification *in situ* by the pH of these pre-treatments are not appropriate for increased biosorption of this hydrophobic aromatic compound. Therefore, the pre-treatment in the autoclave was selected for the next biosorbent preparation, giving adsorption comparable with the two frequently used commercial biosorbents, activated charcoal (83.1 ± 0.0 mg NP/g) and chitosan (56.3 ± 0.1 mg NP/g) (Table 1).

Biosorption of NP exhibited an uptake capacity over 78% and 85% with wide initial pH ranges of 3.1-10.0 and 5.7-7.5, respectively. Maximal NP removal of 87% was obtained at an initial pH 6.6. At initial pH 2.3, however, the NP uptake decreased to 62%. pH solutions at equilibrium under specified conditions in this work were found approximately to decrease from 5.7-7.5 to 4.0-4.9. Accordingly, NP are considered to be molecular form in the range of pH ≤ 7.0 (its pKa = 10.28) (Fan *et al*., 2008). Therefore, NP effectively adsorbed onto fungal biomass in the form of molecules rather than phenolate anion derivatives. The molecular interactions, i.e. hydrogen bonding, hydrophobic interaction and Van der Waals forces could play an important role for the NP adsorption. Neither positive nor negative charges resulting from the biosorbent and pH solution is attractive through electrostatic force for NP biosorption. Nadavala *et al*. (2009) described both phenol and o-chlorophenol existing predominantly as neutral species at pH 7.0. Their interaction with the chitosan-calcium alginate blended beads is considered mainly as non-polar, and the forces responsible for adsorption are physical van der Waals forces.

4.3 Properties of the dead beads

There are a number of immobilisation methods using dead grilled fungal biomass encapsulated in polymer matrix, including calcium alginate and polyvinyl alcohol (Wu and Yu, 2007). In the present study, asexual spores of *R. arrhizus* were trapped into chitosan beads by a liquid curing method in the presence of TPP, and then cultivated for 5 days for complete spore germination. After this period, the hyphae would convert to a sporulation cycle. The bead surface was found to have homogeneously distributed exuberant mycelia inside, and outward growing mycelia covering the whole particle surface. The dry weight of immobilised fungus in the support was 9.7×10^{-4} g/bead. The dried chitosan-immobilised fungal beads had a diameter of approximately 4 mm with a spherical shape which was completely different from the 1-1.5 mm diameter dried plain beads. It also improves the affinity of the biosorbent for the solute by providing directly exposure without any barriers. The dead beads were also stronger and more stable than plain chitosan beads when immersed in acid solution (data not shown), even at pH = 1.

4.4 Evaluation of adsorption isotherms

To model NP biosorption and gain a better understanding of the sorption process, the four adsorption isotherms, Eq.(1-4) were compared to the experimental data for fit. The adsorption isotherm constants with the corresponding correlation coefficients, Eq.(14) and non-normalised RMS, Eq.(15) for each model are presented in Table 2. Although linear regression has been the most commonly used method to obtain the parameters and determine the fit of the kinetic expressions, non-linear regression provides a better measure of fit (Kumar, 2007). As compared to non-linear analysis, the correlation coefficients (r^2) of 0.8912 (Redlich-Peterson), 0.9320 (Freundlich) and 0.7561 (Langmuir), except that for the non-linearized Fritz-

Schlüender, were obtained from the fitting parameters by linear regression. From the results shown in Table 2, the four-parameter isotherm models of Fritz-Schlüender gave the best fit with r^2 = 0.9984, followed by the three- and two-parameter isotherm models of Redlich-Peterson (r^2 = 0.9302), Freundlich (r^2 = 0.9287) and Langmuir (r^2 = 0.9271). Yang and Al-Duri (2005) also observed the superiority of the Fritz-Schlüender model over the other models for biosorption of three reactive dyes onto activated carbon. Based on the Freundlich isotherm plot, the adsorption capacity (K_F) was found to be 30.25 mg/g with an adsorption intensity (n) of 1.87. These were similar values to those for the biosorption of pentachlorophenol onto live *R. arrhizus* which has a K_F of 32.13 mg/g and n of 1.79 (Tsezos and Bell, 1989). The high value of the maximum adsorption capacity, Q_0 of 312.17 mg/g and the low value of the Langmuir constant, b of 0.05 L/mg were obtained with the Langmuir isotherm. In general, a small value of b indicates that the adsorbate has a high binding affinity for the biosorbent (Arica *et al*., 2003). A similar observation was reported for 2,4-dichlorophenol biosorption onto free and calcium alginate immobilised biomass of white-rot fungus *Phanerochaete chrysosporium* with b values of 0.039 and 0.053 L/mg, respectively (Wu and Yu, 2007). The values of K_F and Q_0 also indicate the great affinity for NP by the beads in this study.

4.5 Evaluation of adsorption kinetics

The rate constants for the pseudo first-order (K_1) and pseudo second-order (K_2) sorption reactions were obtained by plotting the non-linear curves fitting Eq.(5) and (6). Kinetic rate constants for NP uptake by the dead beads are presented in Table 3. From the correlation coefficients, the experimental adsorption data gave a better fit to pseudo first-order in the concentration range of 58.62-189.91 mg/L. The

corresponding kinetic models are plotted in Fig 2. Using Eq.(7), the plots of intraparticle diffusion with NP uptake versus *t* at different initial NP concentrations (20.12-245.15 mg/L) are shown in Fig 3. The plots were not linear over the whole time range, implying that more than one process affected the adsorption. Three linear regions better describe the intraparticle diffusion when the initial concentration of NP was in the range 58.62-245.15 mg/L. The initial linear sections have steeper slopes than the subsequent sections. The multi-linearity of the plots can be compared to the three steps of acid dye adsorption onto chitosan reported by Cheung *at al*. (2007). The first, steeper section was attributed to the diffusion of solute through the solution to the external surface of the adsorbent, or the boundary layer diffusion of solute molecules. The second section was attributed to the gradual adsorption stage with diffusion into the mesopores, where intraparticle diffusion was the rate limiting process. The third portion was attributed to the final equilibrium stage for which the intraparticle diffusion started to slow due to the extremely low solute concentration remaining in the solution, and relates to adsorption of the solute into micropores. The slopes of the linear sections indicate the rates of adsorption, a shallower slope corresponding to a slower adsorption process. Thus, it can be implied that the rate-controlling step of NP adsorption was essentially intraparticle diffusion. In addition, relatively low to moderate levels of initial NP concentration (20.12-189.91 mg/L) induced adsorption into micropores as observed from the nearly parallel third section of the plots. The intraparticle diffusivity (*D*) and intraparticle diffusion rate constant (k_p) significantly increase with increased initial NP concentration (Table 4). On the other hand, using a shrinking core model and plotting *F(X)* against α shows significant linear relationships (Fig. 4b), as compared to plotting *X* against α (Fig. 4a). The diffusivity values are in the range of 2.37×10^{-4} to 1.89×10^{-4} $cm^2 s^{-1}$. Clearly, this

implies that intraparticle diffusion is the rate controlling step for the NP biosorption in this work. Although intraparticle diffusion and shrinking core models can describe the biosorption process for NP uptake by the dead beads reasonably well, an initial NP concentration was quite limited lower than approximately 200 mg/g (Fig. 4).

4.6 Desorption kinetics

Desorption studies elucidate the mechanism of adsorption and recovery of NP from water, its interaction with the adsorbent. The adsorbed NP remains mostly stable on the adsorbent and can be desorbed using methanol. It can be seen that the desorption process of NP can well described by a pseudo second-order model using a non-linear regression method (Fig. 5). This was evident from the high r^2 value of 0.9997 and low non-normalised RMS value of 5.2708 as shown in Table 3. NP desorption by methanol also occurred rapidly (K_2 = 4.98x10^{-3} g/mg min). Although, it has been reported that distilled water (Wu and Yu, 2007), $CaCl_2$ solution (Benoit *et al*., 1998) and $NaNO_3$ solution (Daughney and Fein, 1998) can be used to desorb solutes from phenol-loaded and chlorophenol-loaded biomass, using methanol as the desorbing agent allows for easy regeneration as it can be separated from nonylphenol by vapourisation. The NP waste can then be further degraded by chemical or physical treatments (Maniero *et al*., 2008). The regenerated dead beads are also reusable and, from this study, active in four batches (Fig. 6). The weight loss of dead beads was 43% by the end of the fifth batch use.

5. Conclusion

The use of chitosan-immobilised beads was effective for an innovative treatment of low soluble recalcitrant pollutant from wastewater. The fungal dead

biomass could be prepared readily on a commercial scale as an alternative low-cost biosorbent for use in wastewater treatment plants. In this work, the dead beads were pretreated with moist heat which substantially increased their capacity of NP biosorption. Equilibrated NP adsorption with the dead beads best fitted the Fritz-Schlüender isotherm. A maximal monolayer capacity of the dead beads was over 312 mg/g. The rate of NP biosorption was rapid in the first 40 min of contact time. The kinetics for adsorption of NP onto the dead beads was well described by the pseudo first-order equation, while that for desorption was well described by the pseudo second-order one. Both intraparticle diffusion and shrinking core models were found suitably consistent with the adsorption experimental data, especially at the NP concentration less than 200 mg/L. The regeneration of used dead beads with methanol was effective for at least 4 batch cycles in this study. As mentioned, the production of the dead beads and their possible reuses provides an alternative biosorbent for NP removal, as well as for other hydrophobic aromatic recalcitrant pollutants in wastewater.

6. References

Ahel, M., McEvoy, J., Giger, W. 1993. Bioaccumulation of the lipophilic metabolites of nonionic surfactants in freshwater organisms. Environ. Pollut. 79, 243-248.

Aksu, Z. 2001. Biosorption of reactive dyes by dried activated sludge: equilibrium and kinetic modeling. Biochem. Eng. J. 7, 79-84.

Aksu, Z. 2005. Application of biosorption for the removal of organic pollutants: a review. Process Biochem. 40, 997-1026.

Aksu, Z., Balibek, E. 2007. Chromium (VI) biosorption by dried *Rhizopus arrhizus*: Effect of salt (NaCl) concentration on equilibrium and kinetic parameters. J. Hazard. Mat. 145, 210-220.

Asku, Z., Cagatay, S.S., Gönen, F. 2007. Continuous fixed bed biosorption of reactive dyes by *Rhizopus arrhizus*: Determination of column capacity. J. Hazard. Mat. 143, 362-371.

Arica, M.Y., Arpa, Ç., Ergene, A., Bayramoğlu, G., Genç, Ö. 2003. Ca-alginate as a supper for Pb(II) and Zn(II) biosorption with immobilized *Phanerochaete chrysosporium*. Carbohyd. Polym. 52, 167-174.

Benoit, P., Barriuso, E., Calvet, R. 1998. Biosorption characterization of herbicides, 2,4-D and atrazine, and two chlorophenols on fungal mycelium. Chemosphere 37, 1271-1282.

Cheung, W.H., Szeto, Y.S., Mckay, G. 2007. Intraparticle diffusion processes during acid dye adsorption onto chitosan. Bioresour. Technol. 98, 2897-2904.

Daughney, C.J., Fein, J.B. 1998. Sorption of 2,4,6-trichlorophenol by *Bacillus subtilis*. Environ. Sci. Technol. 32, 749-752.

Ekelund, R., Bergman, A., Granmo, A., Berggren, M. 1990. Bioaccumulation of 4-nonylphenol in marine animals. A re-evaluation. Environ. Pollut. 64, 107–120.

Fritz, W., Schluender, E.V. 1974. Simultaneous adsorption equilibria of organic solutes in dilute aqueous solutions on activated carbon. Chem. Eng. Sci. 29, 1279-1282.

Fan, J., Fan, Y., Pei, Y., Wu, K., Wang, J., Fan, M. 2008. Solvent extraction of selected endocrine-disrupting phenols using ionic liquids. Sep. Puri. Technol. 61, 324-331.

Fu, Y., Viraraghavan, T. 2001. Fungal decolorization of dye wastewaters: a review. Bioresour. Tech. 79, 251-262.

Granmo, A., Ekelund, R., Magnusson, K., Berggren, M. 1989. Lethal and sublethal toxicity of 4-nonylphenol to the common mussel. Environ. Pollut. 59, 115–127.

Helander, I.M., Nurmiaho-Lassila, E.L., Ahvenainen, R., Rhoades, J., Roller, S. 2001. Chitosan disrupts the barrier properties of the outer membrane of gram-negative bacteria. Inter. J. Food Microbiol. 71, 235-244.

Ho, Y.S., Mckay, G. 1999. Pseudo second-order model for sorption processes. Process Biochem. 34, 451-465.

Ho, Y.S., Mckay, G. 2000. The kinetics of sorption of divalent metal ions onto sphagnum moss peat. Water Res. 34, 735-742.

Kapoor, A., Viraraghavan, T. 1995. Fungal biosorption-an alternative treatment option for heavy metal bearing wastewaters: a review. Bioresour. Technol. 53, 195-206.

Kapoor, A., Viraraghavan, T. 1998. Removal of heavy metals from aqueous solutions using immobilized fungal biomass in continuous mode. Water Res. 32, 1968-1977.

Kawasaki, N., Araki, M., Nakamura, T., Tanada, S. 2001. Inclusion behavior of 4-nonylphenol into cyclodextrin derivatives. J. Colloid Inter. Sci. 238, 215–218.

Kim, J., Korshin, G.V., Velichenko, A.B. 2005. Comparative study of electrochemical degradation and ozonation of nonylphenol. Water Res. 39, 2527-2534.

Kumar, K.V. 2007. Pseudo second-order models for the adsorption of safranin onto activated carbon: Comparison of linear and non-linear regression methods. J. Hazard. Mat. 142, 564-567.

Lagergren, S. 1989. About the theory of so-called adsorption of soluble substances. Kungliga Svenska Vetenskapsakademiens Handlingar, Band 24, 1-39.

Lavenspiel, O. 1972. Chemical Reaction Engineering. John Wiley & Sons. 2nd ed., 21-32, 69-71, 357-408.

Maniero, M.G., Bila, D.M., Dezotti, M. 2008. Degradation and estrogenic activity removal of 17β-estradiol and 17α-ethinylestradiol by ozonation and O_3/H_2O_2 . Sci. Total Environ. 407, 105-115.

Nakada, N., Tanishima, T., Shinohara, H., Kiri, K., Takada, H. 2006. Pharmaceutical chemicals and endocrine disrupters in municipal wastewater in Tokyo and their removal during activated sludge treatment. Water Res. 40, 3297-3303.

Nadavala, K.S., Swayampakula, K., Boddu, M.V., Abburi, K. 2009. Biosorption of phenol and o-chlorophenol from aqueous solutions on to chitosan–calcium alginate blended beads. J. Hazard. Mat. 162, 482–489.

Nevskaia, D.M., Guerrero-Ruiz, A. 2001. Comparative study of the adsorption from aqueous solutions and the desorption of phenol and nonylphenol substrates on activated carbons. J. Colloid Inter. Sci. 234, 316-321.

Pluemsab, W., Fukazawa, Y., Furuike, T., Nodasaka, Y., Sakairi, N. 2007. Cyclodextrin-linked alginate beads as supporting materials for *Sphingomonas cloacae*, a nonylphenol degrading bacteria. Bioresour. Technol. 98, 2076-2081.

Preetha, B., Viruthagirl, T. 2007. Batch and continuous biosorption of chromium (VI) by *Rhizopus arrhizus*. Sep. Puri. Technol. 57, 126-133.

Singh, A., Kumar, D., Gaur, J.P. 2008. Removal of Cu(II) and Pb(II) by *Pithophora oedogonia*: Sorption, desorption and repeated use of the biomass. J. Hazard. Mat. 152, 1011-1019.

Tsezos, M., Bell, J.P. 1989. Comparison of the biosorption and desorption of hazardous organic pollutants by live and dead biomass. Water Res. 23, 561-568.

Wu, J., Yu, H.Q. 2007. Biosorption of 2,4-dichlorophenol by immobilized white-rot fungus *Phanerochaete chrysosporium* from aqueous solutions. Bioresour. Technol. 98(2), 253-259.

Yang, X.Y., Al-Duri, B. 2005. Kinetic modeling of liquid-phase adsorption of reactive dyes on activated carbon. J. Colloid Inter. Sci. 287, 25-34.

6. Acknowledgements

This work was supported by Thailand Research Fund (TRF) under the research grants "*MRG5080420*" and *"RPUS-I251A13001"* awarded in 2007 and 2008, respectively. The authors are grateful to the Faculty of Liberal Arts and Science and the Faculty of Agro-Industry, Kasetsart University, for facilitating the research, and additional Wilhelm J. Holzschuh of the Faculty for proof reading the manuscript.

Figure captions

Fig. 1 Typical UV-vis spectrum of NP before (—) and after (----) treatment with fungal grill for 1 hour.

Fig. 2 Adsorption kinetics of nonylphenol by the dead beads described with the pseudo first-order model Eq.(5).

Fig. 3 Intraparicle diffusion kinetics for nonyphenol biosorption on the dead beads (multi-linearity) described with Eq.(7).

Fig. 4 Shrinking core model for (a) external film diffusion control and (b) particle diffusion control.

Fig. 5 Comparison of two desorption kinetic models for NP removal by the dead beads. Curve fitting performed with SigmaPlot 11.0 (Systat Software Inc., USA).

Fig. 6 Desorption efficiency of the dead beads after repeated NP biosorption and NP desorption with methanol.

Table 1 Nonylphenol* biosorption of *Rhizopus arrhizus* TISTR 3610 treated with different mycelial preparations.

Biomass/Biosorbent	NP uptake (mg/g)
Pre-treatment	
Untreated	54.4 ± 11.9
Autoclaved (121^{o}C, 15 min)	73.7 ± 1.0
1M H_2SO_4 for 1 hour	49.8 ± 5.1
1N NaOH for 1 hour	37.1 ± 0.0
1N NaOH at 121^{o}C for 15 min	4.5 ± 3.4
10% (v/v) formaldehyde for 1 hour	68.3 ± 0.4
Dried at 50^{o}C for 24 hours	61.2 ± 7.9
Commercial biosorbents	
Activated charcoal	83.1 ± 0.0
Chitosan	56.3 ± 0.1

* Initial NP concentration of 100 mg/L, performed at 100 rpm, at 30^{o}C for 1 hour.

Table 2 Parameters from fitting the adsorption equilibrium data to various isotherm models

Langmuir constants	
Q_0 (mg/g)	312.17
b (L/mg)	0.05
r^2	0.9271
Non-normalised RMS	20.4009
Freundlich constants	
K_F	30.25
N	1.87
r^2	0.9287
Non-normalised RMS	18.5402
Redlich-Peterson constants	
K_R	180.94
α_P	5.26
β	0.49
r^2	0.9302
Non-normalised RMS	18.4794
Fritz-Schluender constants	
K_S	46.87
a_s	0.67
b_1	0.74
b_2	0.35
K_S/ a_s	70.47
r^2	0.9984

Non-normalised RMS	18.4617

Note: Parameters determined using non-linear regression in Microsoft® Excel (Microsoft Corporation, USA).

Table 3 Kinetic parameters for pseudo first-order and pseudo second-order biosorption and desorption of NP using dead beads.

	Nonylphenol		Pseudo first-order rate				Pseudo second-order rate			
	C_0 (mg/l)	q (mg/g)	K_1 (min^{-1})	q_e (mg/g)	r^2	Non-normalised RMS	K_2 (g/mg min)	q_e (mg/g)	r^2	Non-normalised RMS
Biosorption	20.1156	19.4558	0.10227	16.4679	0.6726	2.0072	$1.03x10^{-2}$	17.2494	0.5742	2.2347
	58.6191	55.9184	0.03606	54.3062	0.9878	1.7437	$7.41x10^{-4}$	61.3428	0.9921	1.3298
	115.3538	100.5443	0.02267	102.5006	0.9107	10.2708	$1.91x10^{-4}$	122.9755	0.8635	12.7894
	189.9116	171.9728	0.02705	171.2495	0.9150	16.1795	$1.47x10^{-4}$	200.9999	0.8753	21.0549
	245.1497	207.4150	0.01119	224.9302	0.8597	30.8957	1.76×10^{-5}	338.0162	0.6926	50.3715
Desorption	-	145.6420	0.40945	138.1793	0.5655	29.5331	$4.98x10^{-3}$	145.8314	0.9997	5.2708

Note: Parameters determined using non-linear regression in Microsoft® Excel (Microsoft Corporation, USA).

Table 4 Intraparticle diffusion and shrinking core coefficients

Initial concentration of NP (mg/L)	Intraparticle diffusion			Shrinking core model		
	Slope	k_p mg/(g. $min^{0.5}$)	Diffusion coefficient (cm^2/s)	Slope	C^0 (mg/L)	Diffusion coefficient (cm^2/s)
20.12	1.21	$9.79x10^{1}$	0.15	$1.89x10^{-3}$	1.03	$2.37x10^{-4}$
58.62	3.76	$9.32x10^{2}$	1.67	$5.89x10^{-4}$	2.95	$2.80x10^{-4}$
115.35	8.38	$3.30x10^{3}$	6.50	$4.41x10^{-4}$	5.30	$3.65x10^{-4}$
189.91	12.30	$8.80x10^{3}$	15.75	$2.21x10^{-4}$	9.07	$2.98x10^{-4}$
245.15	14.70	$1.31x10^{4}$	24.01	$1.22x10^{-4}$	10.94	$1.89x10^{-4}$

Bead dosage = 0.1 g, NP solution volume = 100 ml, bead amount = 18 beads

Note: Parameters determined using non-linear regression in Microsoft® Excel (Microsoft Corporation, USA)

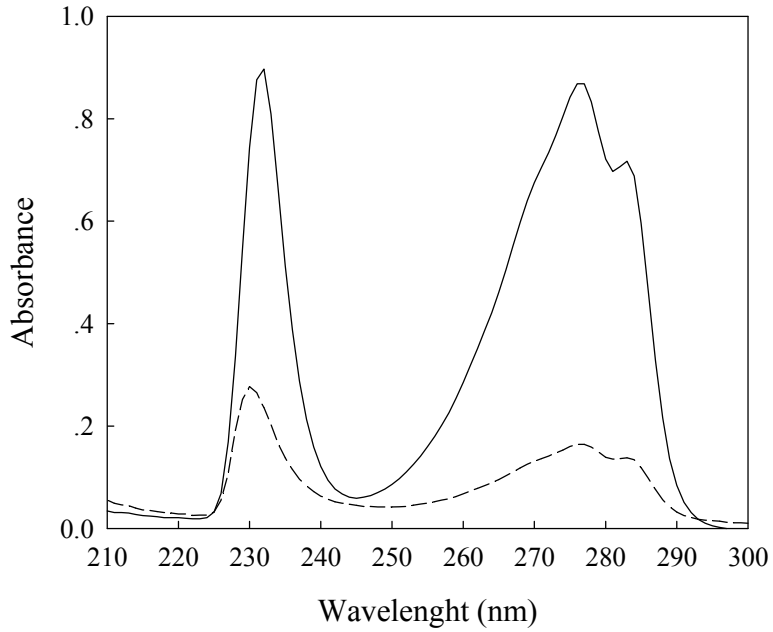

Fig. 1 Typical UV-VIS spectrum of NP before (—) and after (----) treatment with fungal grill for 1 hour.

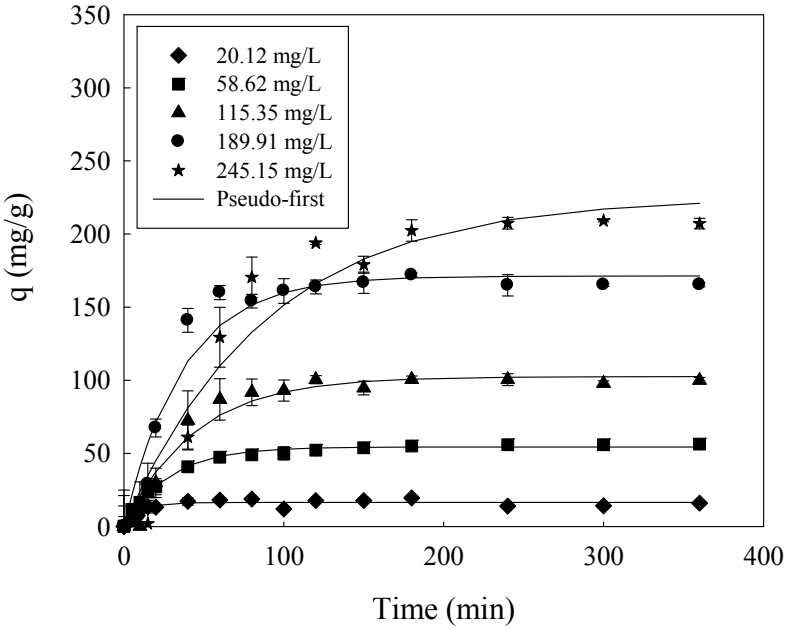

Fig. 2 Adsorption kinetics of nonylphenol by the dead beads described with the pseudo first-order model Eq.(5).

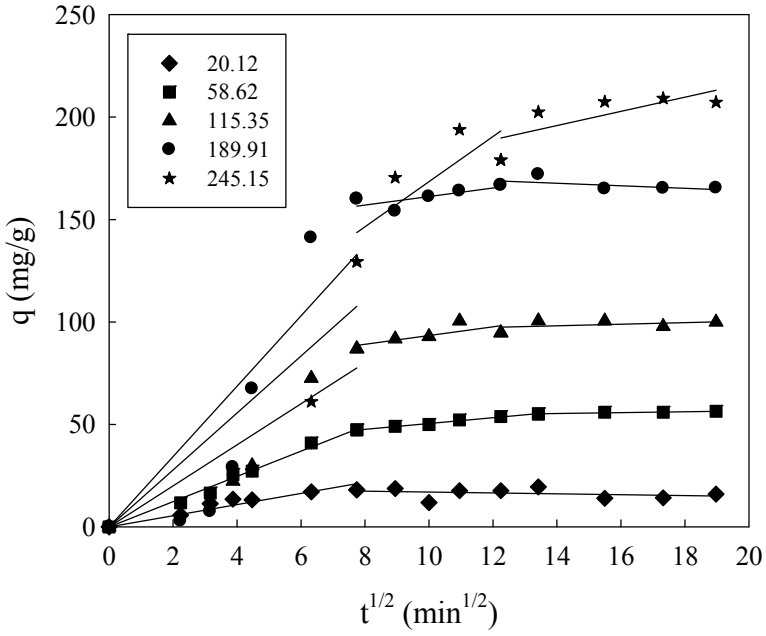

Fig. 3 Intraparicle diffusion kinetics for nonyphenol biosorption on the dead beads (multi-linearity) described with Eq.(7).

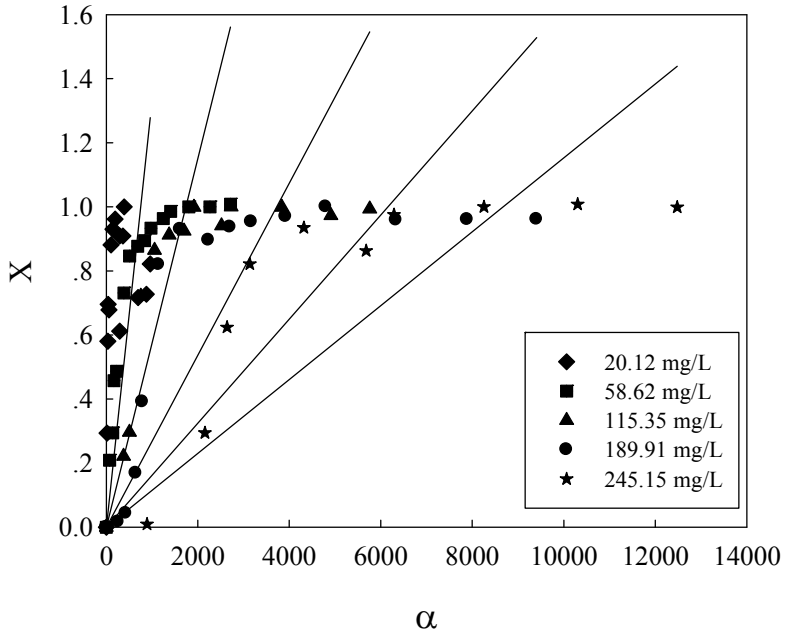
1.6
1.4
1.2
1.0
.8
.6
.4
.2
0.0
X
0
2000
4000
6000
8000
10000
12000
14000
α
20.12 mg/L
58.62 mg/L
115.35 mg/L
189.91 mg/L
245.15 mg/L

Fig. 4a

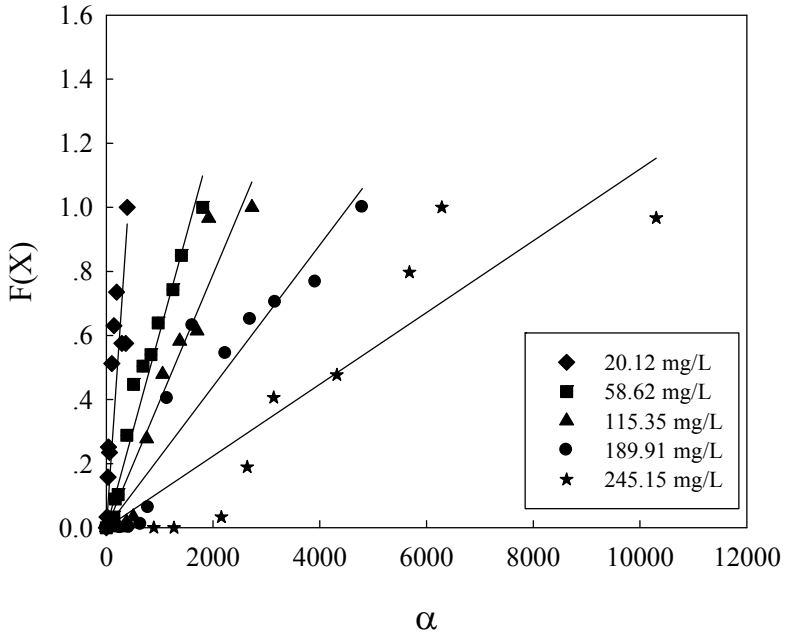
1.6
1.4
1.2
1.0
.8
.6
.4
.2
0.0
F(X)
0
2000
4000
6000
8000
10000
12000
α
20.12 mg/L
58.62 mg/L
115.35 mg/L
189.91 mg/L
245.15 mg/L

Fig. 4b

Fig. 4 Shrinking core model for (a) external film diffusion control and (b) particle diffusion control.

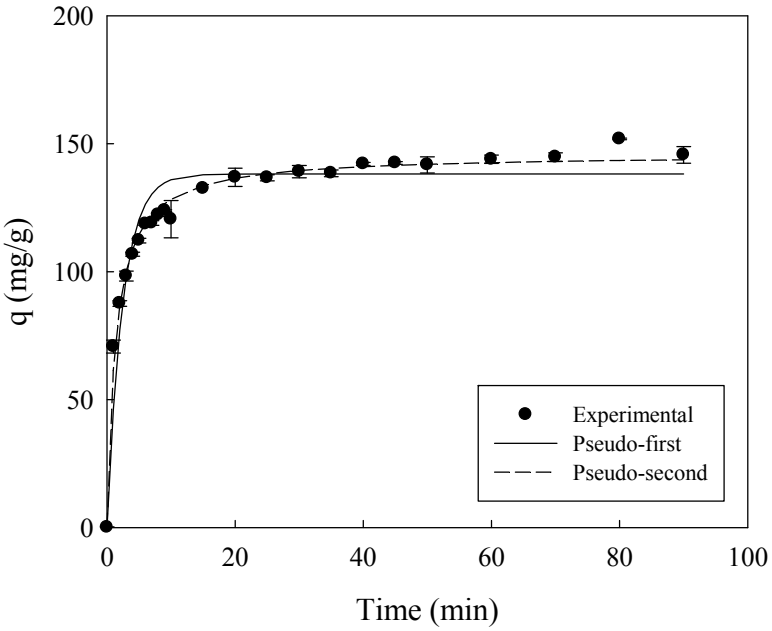

Fig. 5 Comparison of two desorption kinetic models for NP removal by the dead beads. Curve fitting performed with SigmaPlot 11.0 (Systat Software Inc., USA).

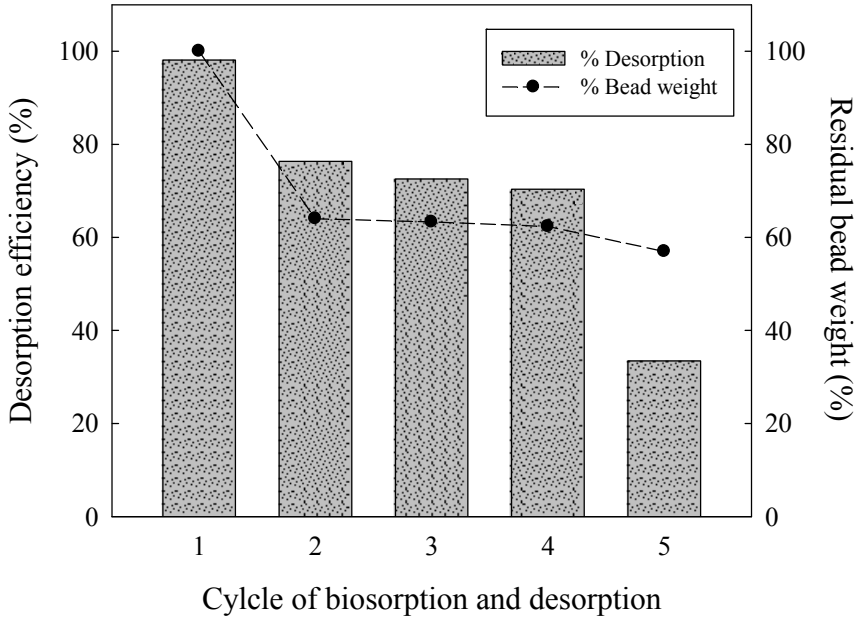

Fig. 6 Desorption efficiency of the dead beads after repeated NP biosorption and NP desorption with methanol.